Arab J. Nucl. Sci. Appl., Vol. 56, 3, 129-144 (2023)

ISSN 1110-0451

Arab Journal of Nuclear Sciences and Applications

Web site: ajnsa.journals.ekb.eg

(E S N S A)

Evaluation of Gamma Ray Attenuation Properties of Normal Concrete with some Nano Materials Using Monte Carlo Simulation and Experimental Measurements

Rasha A. El-Sadany[1] *, Sherif H. Al-Tersawy[2], Khaled Aly Metwally[3], W- Elgamaal[4]

(1) *Radiation Engineering Department, National Center for Radiation Research and Technology, Egyptian Atomic Energy Authority, Cairo, Egypt. (E-Mail: rasha_sadani@yahoo.com).*

(2) *Civil Engineering Department, Higher Technological Institute (HTI), 10th of Ramadan City, Egypt (E-Mail: al_tersawy@hotmail.com).*

(3) *Department of Construction and Building, Higher Institute of Engineering, Giza, Egypt (Email: khaledalymetwally@gmail.com).*

(4) *Egyptian Nuclear and Radiological Regulatory Authority- Cairo, Egypt (E-Mail: wgammal66@yahoo.com).*

ARTICLE INFO

Article history:

Received: 10th Nov. 2022

Accepted: 11th Jan. 2023

Keywords:

Radiation Shielding;

Nano Materials;

Monte Carlo;

Mechanical;

Microstructure;

XRD.

ABSTRACT

The linear attenuation coefficient of normal weight concrete containing nanoparticles has been simulated using Monte Carlo transport code MCNP5 to evaluate their shielding performance. The outcomes of the numerical simulations were compared to the experimental samples computed with Cesium 137 (0.662 MeV) and XCOM program results. Three different nanoparticles mainly nano silica (NS), nano ceramic (NC), and nano metakaolin (NMK), and their hybridization were used in the present research. Slump test, density, water absorption, compressive strength and tensile strength were investigated. Moreover, the scanning electron microscopy technique (SEM), X ray diffraction analysis (XRD) were used to prove the improvement in the microstructure of concrete as a result of the use of NS, NC, NMK, and their hybridization. The results in the present study indicate that the inclusion of single nanomaterials as a replacement of cement improves the mechanical, physical, properties and the linear attenuation coefficient of concrete, while the results of the hybrid nano inclusion showed a slight improvement of the properties of concrete. In addition, the results of the simulation of the linear attenuation coefficient using the Monte Carlo simulation were in good agreement with the experimental and XCOM program results.

1-INTRODUCTION

The utilization of nano silica in concrete mixture has appeared improvement in compressive, flexural, tensile and flexural strength of concrete. When adding nano silica as a replacement of cement, it can generate nano crystal of C-S-H gel after hydration. These nanocrystals are absorbed in the micro pores of the cement concrete, hence, the improvement in the permeability and strength of the concrete can be achieved [1]. A 70 % increase in compressive strength can be achieved when the cement is replaced by 4% NS [2]. The effect of different dosages of nano silica on properties of concrete was investigated by Nazari and Riahi [3]. They concluded that the improvement in compressive strength of concrete will be achieved due to the improvement in the microstructural of concrete. In a previous study[4], it was concluded that the concrete containing 25% fly ash and 1% nano silica gave the highest compressive strength when compared to other mixes. Another study [5] obeved that while improvement in compressive strength and durability properties were obtained when nano silica was added to concrete containing 25% recycled aggregate, the improvement in tensile strength was achieved in concrete with 50% recycled aggregate. Mohd et al. [6] investigated the influence of nano silica in mortar and cement paste regarding porous concrete pavement. They concluded that the incorporation of nano silica in cement paste and mortar with the right composition will improve their mechanical properties. The positive impacts of utilizing nano silica in concrete, cement paste and mortar have appeared in earlier publications [7-10]. Ghafarti et al. [11] and Tawfik et al. [12] achieved the best performance of concrete when using 3 wt. % of nano silica. In another work [13], the authors concluded that incorporating 2% NS and 8% micro silica as partial replacements of cement can improve the tensile and compressive strength for normal strength and high strength concrete. In addition, when using the hybrid silica (micro and nano), the $Ca(OH)_2$ crystals disappeared, and the cement matrix became more dense than the control mix.

Corresponding author: rasha_sadani@yahoo.com
DOI: 10.21608/ajnsa.2023.173903.1678

Metakaolin (MK) is a Kaolinite calcined clay, it can be used in concrete as supplementary cementing materials (as partially replacement of cement) [14, 15]. The particle size of metakaolin is smaller than cement particles, but not as fine as silica fume. Metakaolin has been known as a very reactive pozzolan, for this reason, the incorporation of MK in concrete will improve the mechanical properties, permeability and chemical resistance. In addition, metakaolin improves the packing of particles in the matrix through its fine particles, [16]. The surface area of nano metakaolin can be increased by 2- 8 times when the MK changed to nano metakaolin (NMK), and it is possible to minimize NMK into smaller particles depending on the transformation process. NMK is similar to MK in shape and surface texture [17]. On the other hand, Morsyet et al. [18], investigated the addition of nano metakaolin in cement mortar, they found that the improvement in the compressive strength and the tensile strength of mortar can be achieved when using 2% up to 8% NMK as replacement of cement. Shoukry et al. [19] showed that the peak of X-ray diffraction intensity and calcium hydroxide (CH) content were decreased slightly when increasing the amount of NMK replacement, although the calcium silicate hydrate (C-S-H) peak value showed a growing trend. The CH content of cement paste was reduced by 6.7% due to the increase of NMK [20]. Moreover, Shoukr et al. [19, 20] studied the influence of incorporates of NMK at a rate from 2 to 10% on the properties of high-volume vermiculite blended white Portland cement (WPC). WPC was replaced with 70 vol% expanded vermiculite (EVM), they concluded that the increase in compressive and tensile strength were achieved by 57 and 59%, respectively when using 10% NMK replacement of cement. On the other hand, Nithya et al. [21] concluded that the use of 1% nano metakaolin as a replacement of cement will give the maximum compressive strength than a 10% metakaolin as a replacement of cement. Additionally, Xie et al. [22] found that the compressive strength gradually increases with the increase of NMK at a constant recycled aggregate concrete. The 28-day compressive strength of recycled concrete increased with increasing the NMK content when the replacement rate of recycled aggregate was constant. On the other hand, the slump of concrete containing 9% NMK was reduced by 15.7 % while the setting time increased at 2% NMK, and then decreased at 20% NMK.

Ceramic nanoparticles are a form of nanoparticles made up of ceramics, characterized by nonmetallic solids, heat-resistant and inorganic material which can be made up of nonmetallic and metallic compounds. The substance has its own set of characteristics. Macroscale ceramics are stiff, brittle and they break when struck. On the other hand, ceramic nanoparticles can perform a wider range of functions, such as pyroelectric, dielectric, piezoelectric, ferroelectric, ferromagnetic, superconductive, electro-optical and magneto resistive [23]. Ceramic nanoparticles have been utilized to deliver drugs in a variety of diseases, such as cancer chemotherapy, glaucoma and bacterial infections, [24]. Among the researches which investigated nano ceramic, Tawfik et al. [12] who studied the effect of nanoceramic (NC) and nano silica (NS) on the properties of concrete, they found that using NC up to 6%, NS up to 3% and hybrid of NS and NC can improve the mechanical properties of concrete. However, Li et al. [25] showed that the improvement in compressive strength will be achieved when using micro ceramics as a replacement of cement. Singh et al. [26] used seven types of concrete which were used in nuclear reactor facilities. They concluded that the results of attenuation properties from experimental data, XCOM program and MCNP for energies 1.5, 2, 3, 4, 5 and 6 MeV are in very good agreement. Moreover, high-density concrete was investigated for mega voltage photon beam spectra for various energies (4, 6, 10, 15, and 18 MeV) of the Varian linac and Co^{60} gamma rays and were simulated using Monte Carlo method by Khaldari et al. [27]. They concluded that the attenuation of high-energy photons was affected by both density of the concrete and atomic number. Moreover, they found that the relation between the density and the attenuation coefficient was not totally linear. McDowall [28] studied the shrinkage of concrete subjected to a dose of 1.14 × 102 Gy/hr for 320 days. He found that the shrinkage of the irradiated samples was three times more than that of the non-irradiated samples. He concluded that the increase in shrinkage was due to the radiolysis of water of hydration in the concrete which would cause losses in strength. According to the results of the experimental data and computer simulation, alloy steel added to concrete has the best shielding properties, however concrete with various fillers added also showed improvement in the shielding ability. It was shown that by increasing the fillers to 6 w%, the improvement in the shielding capability for ordinary concrete against x-ray/gamma ray reached 40~60% [29].

3-EXPERIMENTAL PROGRAM

3.1. Materials

The nano materials used in the present study were nano silica (NS), nano Ceramic (NC), and nano metakaolin (NMK). They were used in a powder form as a partial replacement for cement. NS was brought from Nanotech Egypt for Photo-Electronics, Giza, Egypt, while NMK was brought form Helwan and NC were prepared in Housing and Construction Research Center by crushing the ceramic and grinding it and finally, it was placed in a pooling mail in the Egyptian Atomic Energy Authority, Cairo, Egypt. Ordinary Portland cement (OPC) used in this research was (CEM I/42.5 N) in compliance with ESS 2421/2005 [30]. Mechanical properties of cement are shown in Table(1), chemical composition of the cement and nano materials are shown in Table (2), and physical properties of nano materials are shown in Table (3). The TEM images of the nanoparticles are shown in Figure (1), and their XRD diffractograms are shown in Figure (2). Natural gravel and sand were used in the experimental work. The 10 mm maximum nominal size of gravel was used. The results of testing for both natural gravel and sand are presented in Table (4) according to the ESS 1109/2002 [31]. According to the mix design, the w/c ratio was used as 0.42. The superplasticizer used is a product of Sika Company; Viscocrete 10. It has the following properties: dosage = 0.3–2% by weight of cement, density = 1.08 kg/l, and base = modified polycarboxylates.

Table (1): Mechanical properties of cement

Properties		Measured values
Blaine surface area (cm^2/gm)		2850
Specific gravity		3.15
Soundness (Le Chatelier) (mm)		1.3
Initial setting time min)		120
Finial setting time (min)		160
Compressive strength (MPa)	2 days	22
	28days	51

Table (2): Chemical composition of cement, Nano silica, Nano Metakaolin and Nano Ceramic

Oxide %	Cement	Nano silica	Nano Metakoline	Nano Ceramic
SIO_2	20.89	95.39	89.6	66.57
Al_2O_3	4.78	0.15	0.9	21.6
Fe_2O_3	3.94	1.11	2.0	1.41
CaO	63.01	0.43	.43	2.14
MgO	2.01	0.09	0.09	-
SO_3	2.68	0.05	-	-
K_2O	0.19	0.030	4.55	2.79
Na_2O	0.19	1.790	-	1.41
CL-	0.02	0.71	-	-
TiO_2	3.6	2.9-	1.61	0.7
ZrO_2	--	-	-	1.49
L.O.I.	1.99			

Table (3): Physical properties of Nanoparticle

	NS	NMK	NC
Appearance (Color)	White	Brown	Brown
Appearance (Form)	Powder	Powder	Powder
Solubility	Dispersion into water or ethanol	Dispersion into water or ethanol	Dispersion into water or ethanol
Avg. Size	15-25 nm	7-13 nm	11-17 nm
Density gm/cm^3	1.989	2.5	0.923

Table (4): Properties of gravel .and sand

Test	Sand	Gravel
Specific weight	2.63	2.56
Bulk density(t/m^3)	1.72	1.66
Clay and line dust content (%)	1.4	1.7
Abrasion (Los Angeles)	-	12.6
Impact value (%)	-	10.6
Water absorption (%)	-	1.03

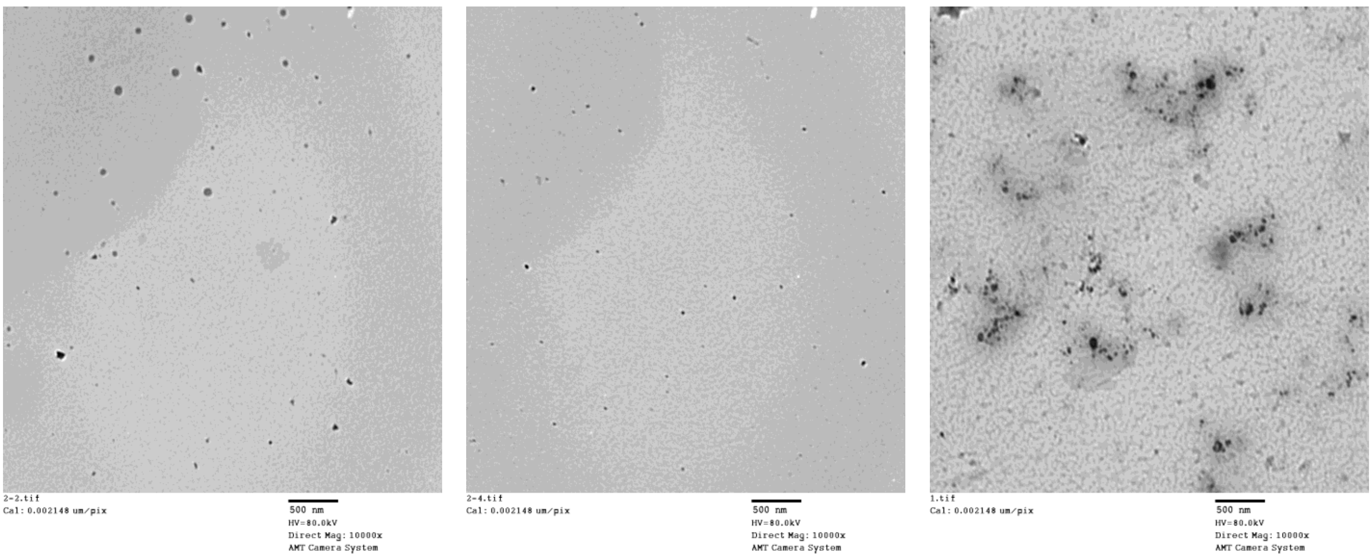

NS ***NMK*** ***NC***

Fig. (1): TEM of nano particles

3-2 Mix Design and Samples preparation

The experimental program is composed of six concrete mixes. It is composed of a control mix and five concrete mixes with three nano materials as given in Table (5), NS, NC, and NMK are the three nano mixes, and the fourth and fifth mixes were hybridization of two types of nano materials (NS+NC) and (NS+NMK). The unsafe utilization of nano particles has dangers to one's wellbeing. To keep away from contact with the nanomaterial, gloves and extraordinary masks with satisfactory filters were used when preparing the samples. The dry contents: cement, gravel and sand were mixed in high-speed mixer for 2 min to obtain a homogenous mix. The nanoparticles were added to the dry contents after being thoroughly dispersed in the mixing water using a high-intensity ultrasonic bath (frequency: 20 kHz) for 15 minutes. At the end, all the contents were mixed in the mixer at a speed of 50 rpm. Three sets of samples were cast for testing in this investigation. For testing the density, water absorption, and compressive strength, the first group was cast in 10x10x10 cm cubes. The second group was cast as cylinders with dimensions of 15 cm in diameter and 30 cm in height for tensile strength testing and radioactivity experiments. To determine the linear attenuation coefficient, the cylinder was cut to various thicknesses. For flexural strength, the third group was cast as a 10x10x50 cm prism. In the casting room, all test specimens were kept at a temperature of 24^0C. They were put into a tank of water until testing of samples after being demolded for 24 hours.

3.3. Testing of Concrete Samples

The following experiments' tests on hardened concrete were carried out in the current study:

3-3-1 Compressive Strength

The test was performed using control compression machine with capacity 200KN according to the Egyptian Standard Specifications ESS 1658/2006 [32]. To determine the concrete compressive strength at different ages, compression tests were performed on concrete specimens in normal conditions at 7 and 28 days.

3-3-2 Tensile Strength

The tensile strength and flexural strength were determined according to the Egyptian Standard Specifications ESS 1658/2006 [32]. The average strength of three samples per mix was reported.

3-3-3 Water Absorption and Density

Water absorption and density were computed according to ASTM C642-97 [33]. In absorption test, first, the specimens were dried in an oven drier at about 110 °C for 24 h. After that, the specimens were cooled to 22 °C and their masses were calculated. This procedure was repeated until the specimen masses were stable, and the dry masses were recorded (W_d). Then, the specimens were removed after 48 hours of immersion in water, their surfaces were thoroughly dried, and their saturated masses were computed (WS). Finally, the water absorption was calculated using the formula % = $(W_S-W_d)/W_d$. The average of three specimens was reported. The average density of three samples per mix was measured.

3-3-4 XRD Testing

The XRD test is a nondestructive test. The samples for this test were cured for 28 days and then ground into powder in order to achieve higher accuracy. The obtained dry hydration samples were subjected to X-ray diffraction (XRD) analysis using a X-ray diffractometer (XRD Shimadzu 6000) employing Cu-Kα radiation (λ = 0.15418 nm, 40 kV, 50 mA) over scanning range 2θ =0° ~ 90° at step width 8° per min. The XRD for nano materials were shown in Figure (3).

Table (5): Composition of Concrete Mixes and results

Mix	Nano %	Cement (kg)	Gravel (kg)	Sand (kg)	Water (kg)	WR (kg)	Nano (kg)	Slump	Compressive strength (kg/cm^2)		Tensile strength (kg/cm^2)	% absorption	Density (kg/m^3)	µ -Mont Carlo (cm^{-1})	µ-Practical (cm^{-1})	µ- XCOM (cm^{-1})
									7 days	28 days						
Con.	Control	350.0	1400	700	147.0	52.6	0.0	12	196	260	25	3.5	2.35	0.179	0.176	0.182
NS	3%	339.5	1400	700	143.0	50.9	10.5	10	210	286	29	3.1	2.39	0.182	0.179	0.185
NC	6%	329.0	1400	700	138.2	49.4	21.0	9	220	290	29	3	2.44	0.186	0.183	0.189
NMK	2%	343.0	1400	700	144.1	51.5	7.0	8	240	319	30	2.8	2.61	0.199	0.196	0.202
NS+NMK	3%+2%	332.5	1400	700	139.7	49.9	31.5	10.5	206	272	26	2.6	2.37	0.181	0.178	0.184
NS+Nc	3%+6%	318.5	1400	700	133.8	47.8	17.5	11	205	272	28	2.7	2.38	0.181	0.179	0.185

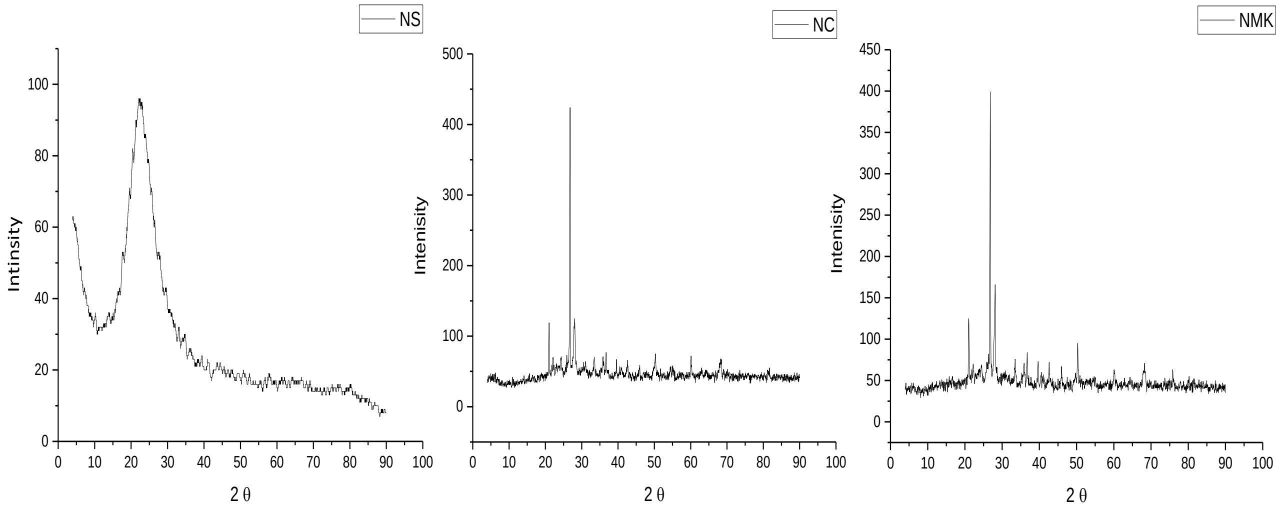

Fig. (2); XRD for nano materials

3-3-5 Microstructure

The Microstructure was examined using SEM analysis that also provided visual clear evidence of the microstructural elements which are responsible for improving the physical and mechanical properties. Samples were morphologically investigated using a scanning electron microscope model ZEISS-EVO 15-UK operating at 25 kV. To prepare the specimen for microstructure analysis, following the strength test, the small specimen containing hardened cement and nano material were removed from crushing specimen and were dried at 50ºC for 1 day and then coated with a thin layer of gold. These analyses were carried out at the National Center for Radiation Research and Technology-Atomic Energy authority- Egypt.

3-3-6 Experimental measurements of shielding properties

The measured samples are prepared in cylindrical forms of 15 cm diameters and five different thicknesses (heights). Six groups of samples are investigated as mentioned in sec. 3-2 and Table (5). Due to the existence of some tolerance, the thickness of each sample was measured at five different locations. Shielding properties of ordinary concrete and concrete with nano materials samples have been investigated through measurement of their linear attenuation coefficients. The measurements are performed by allowing the mono-energetic gamma-rays (661.7 keV) emitted from a Cs-137 point source to penetrate the samples and detected by a 3”x3” NaI(Tl) detector. To reduce the time of measurement, two Cs-137 sources with a total activity of 15 µCi± 3% were placed together. The used gamma ray spectrometer system is composed of a Multichannel Analyzer (Model: 166-USB V2, GBS Elektronik, GmbH Rossendorf), the NaI detector is (Amcrys, type: 12S12/3.VD.PA) and the used software was WinSPEC for spectrum acquisition and analysis. A set of collimators are used to produce a near line beam of gamma radiation. Figure (3) shows the setup of the detection system, the set of collimators, the location of the sample, the gamma source, and the front and rear views of the collimators set. The dimensions and locations of collimators and samples are illustrated in Figure (4). The openings of the set of collimators were aligned using a metallic rod that has almost the same diameter as those of the openings. The measuring time ranges between 950 to 5000 seconds to measure samples of different thicknesses starting from zero (no sample) to about sample with 10 cm. The measuring time was adjusted in such a way to keep statistical error in count rates always less than 3%. Three runs were performed for each sample. Since the concrete samples are normally not homogeneous and there is a recognized tolerance in thickness, the sample was rotated to measure the penetration probability at three different locations for each run. According to Eq.1, the linear attenuation coefficients of the concrete specimens were calculated from the slope of the relation between count and the thickness (cm) [34].

$$\mu = \frac{\ln(I_o/I_x)}{x} \qquad \textbf{(1)}$$

Where:

μ: Linear attenuation coefficient, cm^{-1}

I_0: The count of gamma rays (without absorber)

Ix: The count of gamma rays (at each specimen thickness)

x: Specimen thickness, cm

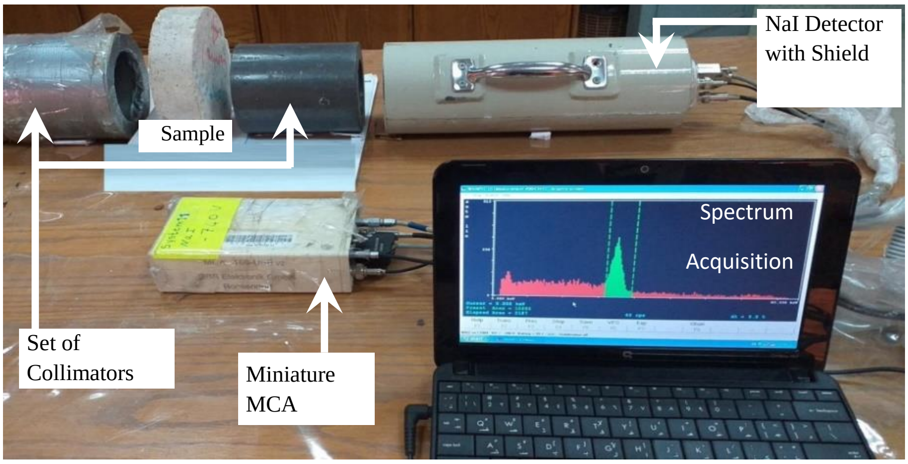

Fig. (3): Setup of the detection system

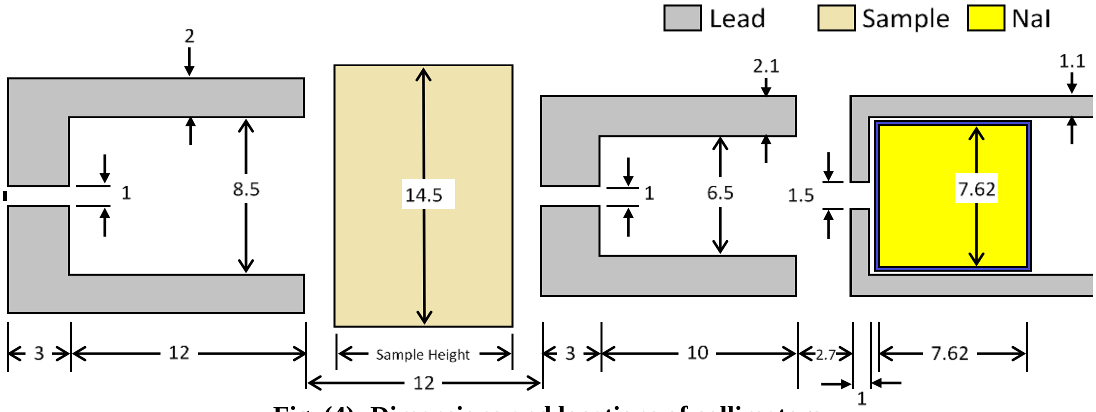

Fig. (4): Dimensions and locations of collimators

Table (6): Fraction of elemental compositions for ordinary concrete and concrete containing nano materials

Element	Atomic Fraction (%)					
	Control	NS 3%	NC 6%	NMK 2%	NS+NMK 3%+2%	NS+NC 3%+6%
H	0.64	0.64	0.64	0.64	0.64	0.64
O	49.64	49.69	49.69	49.67	49.71	49.74
Si	30.49	30.61	30.64	30.56	30.69	30.76
Al	4.58	4.56	5.38	4.56	4.55	4.61
Fe	1.21	1.19	1.17	1.20	1.18	1.15
Ca	8.99	8.82	8.66	8.88	8.71	8.49
Mg	0.26	0.26	0.25	0.26	0.25	0.25
S	0.20	0.19	0.18	0.19	0.19	0.18
Na	1.72	1.73	1.72	1.72	1.72	1.72
K	1.90	1.90	1.92	1.91	1.91	1.92

3-3-5 Theoretical Calculations of linear attenuation Coefficient

Two methods are considered to determine the theoretical linear attenuation coefficients for the samples. They include using the online XCOM database and Monte Carlo calculations.

A) XCOM

The XCOM [35] is an available web database that can be directly used to calculate the mass attenuation coefficient for elements, compounds and mixtures. It performs calculations based on narrow beam penetration probability through homogeneous samples. Consequently, the linear attenuation coefficient for ordinary concrete samples is obtained assuming their homogeneity. The fraction of elemental compositions for ordinary concrete and concrete containing nano materials used in XCOM are given in Table (6).

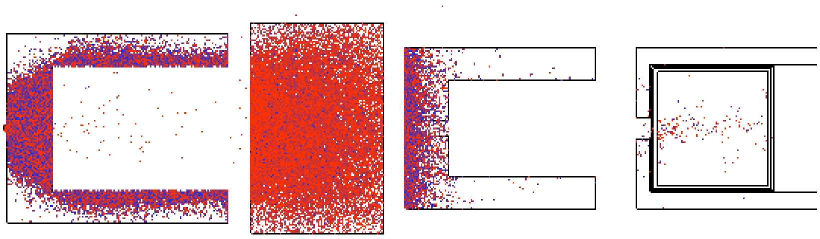

Fig. (5): Exact modeled setup as drawn by the MCNP visual editor with particle collisions

B) Monte Carlo

The MCNP general Monte Carlo Code is used for estimation of the linear attenuation coefficient of ordinary concrete samples, and samples with nanomaterials. Two cases are considered. First, exact modeling of experimental setup for ordinary concrete measurements is carried out to check the model validity. Secondly, ordinary concrete samples with nanomaterials are modeled to determine any changes in the shielding properties.

a) Modeling of experimental setup for ordinary concrete

The experimental setup for ordinary concrete is modeled as shown in Figure (3) using the MCNP Code. Figure (4) shows the dimensions and locations of the used collimators. Figure (5) presents the modeled setup as drawn by the MCNP visual editor. Photon tracks (interactions) are also illustrated in the Figure indicating the exact modeling without any source biasing variance reduction techniques. The MCNP Pulse height tally "F8" is used to calculate the absolute full energy peak efficiency of the detector at the 0.662 MeV gamma-ray energy. Calculation of "F8" tally without a sample, and with samples of different thicknesses allow the determination of μ_l through fitting the exponential absorption relation $I/Io=\exp(-\mu x)$, where Io and I are the intensity of un-attenuated and attenuated radiation in the absorber medium, respectively. Material card is used to define material composition of the ordinary concrete sample by weight fractions as given in Table (7). The number of histories is selected and defined in the MCNP nps card to keep statistical error in MCNP calculations less than 1%. (2e8 35 min uncert 0.5%).

b) Modeling of concrete with nanomaterials

The validated model of ordinary concrete is modified to investigate the effect of nanomaterials. Figure (6) shows a drawing for the MCNP model used to estimate the linear attenuation coefficient for ordinary concrete and concrete with nano materials samples. A mono energetic (0.662 MeV) mono directional (DIR=1) point source is defined in the MCNP SDEF card. A set of lead collimators is considered to define a narrow beam of radiation. Samples with nanomaterials of 15 cm diameter and different heights (1-10 cm) are modeled. Moreover, the MCNP repeated structure geometry feature with the U (universe), FILL, LAT (lattice) associated cards is employed to create the nano-structure material. A lattice of type 2, RHP (Right Hexagonal Prism) is filled with two universes (ordinary concrete and nano-silica), (ordinary concrete and nano-ceramic) and (ordinary concrete and nano-metakaolin) for samples with 3% NS, 6% NC and 2% NMK by mass respectively. However, three universes are used to fill the lattice for samples with hybrid nanomaterials (NS 3%+NC 6%) and (NS 3%+NMK 2%) respectively. Nano materials are defined as spheres of 1.4e-7 cm diameters and densities of 1.989, 2.5 and 0.923 cm^3/g for NS, NMK and NC materials, respectively. The building unit is composed of a hexagonal prism that contains the spheres of nanomaterials. The number of spheres inside a prism is calculated using their volumes and densities relative to the mass of ordinary concrete in the prism. The atomic fractions of the elemental composition for nanomaterials are given in Table (7). Figure (7) shows the repeated structure of the MCNP model created to estimate the linear attenuation coefficients for samples with 3% NS. A three-dimensional drawing created by the 3D Ray Tracing capability of the MCNP for the one building unit of samples with 3% NS is presented in Figure (8). The 3D drawing is treated with a cookie cutter cell to illustrate the nanoparticles inside.

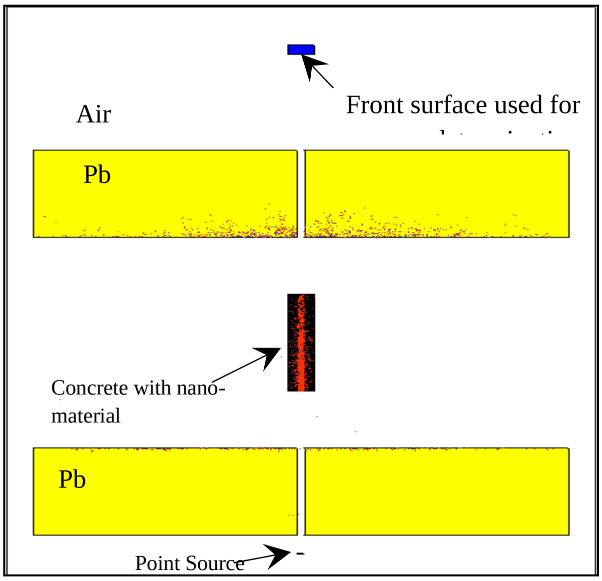

Fig. (6): MCNP model

Table (7): Atomic fractions of elemental composition of nanomaterials

Element	Atomic fraction (%)		
	NS	NMK	NC
O	65.25	64.60	52.40
Si	31.80	29.87	26.00
Al	0.06	0.36	0.26
Fe	0.44	0.80	1.00
Ca	0.22	0.22	0.22
Mg	0.05	1.00	-
S	0.01	-	-
K	0.02	2.91	2.00
Na	1.19	-	1.00
Cl	0.71	-	-
Ti	-	0.23	-
Zn	-	-	1.00

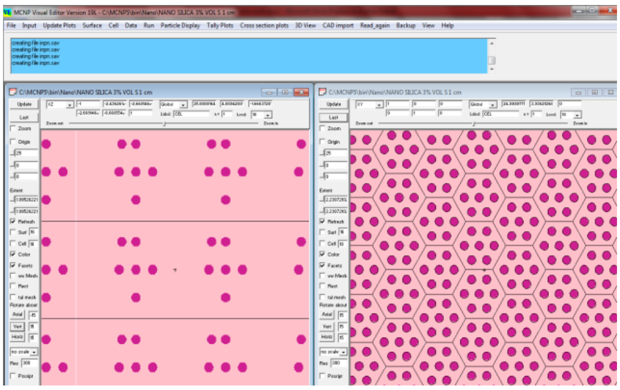

Fig. (7): Repeated structure of the MCNP model

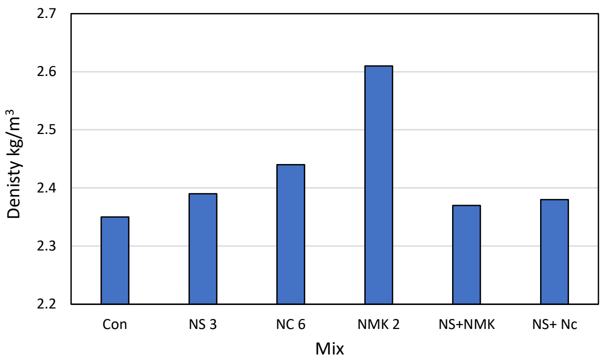

Fig. (8): Tracing capability of the MCNP

4-RESULTS AND DISSECTION

4-1 Properties of Fresh concrete

According to ESS 1658/2006 [32], the concrete's workability is measured in terms of slump. The slump of all mixes is shown in Figure (9). It can be observed that the slump of concrete with nanomaterials was decreased than the control mix by about 16.7, 25, 12.5, and 8.3% for NS, NC, NS+NMK and NS+NC respectively. However, the slump of NMK was decreased by 33.3% compared to the control mix. This may be attributed to the large specific surface area of nano metakaolin which absorbed more water from concrete than nano silica and nano ceramic, which is partially in confirmation of previously reported results [36].

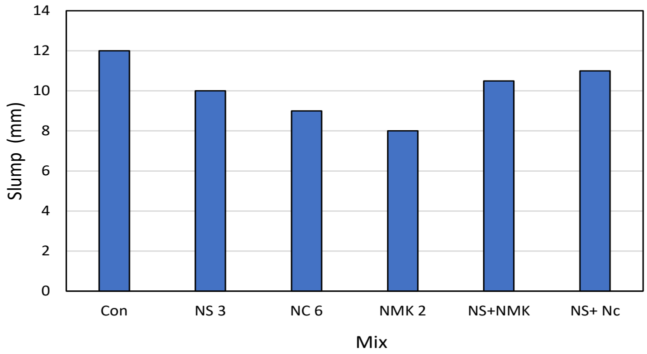

Fig. (9): Slump of concrete mixes

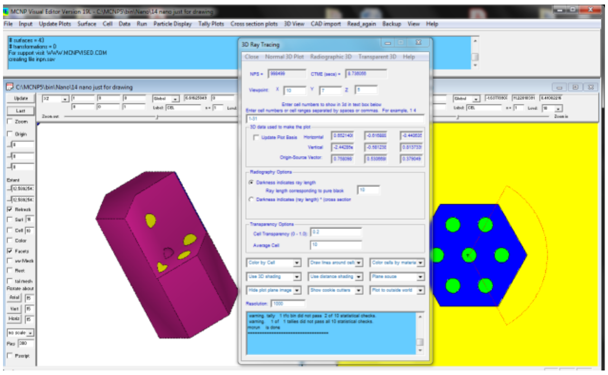

Fig. (10): Density of concrete mixes

4-2 Mechanical Properties of Concrete

4-2-1 Density

The results of density of all mixes are presented in Table (5) and Figure (10). As expected, the NMk mix has a higher density than that of the control, NC, or NS mix. The high density was due to the small size of NMk particles when compared with NC or NS particles as shown in Table (3) which result in a low pour in the mixture of concrete. This is confirmed by SEM micrographs shown in Fig. (21). However, the hydration degree of cement particles increases due to the nucleation of nano ceramic or nano silica and pozzolanic reaction which causes additional hydration products to fill the particles pores resulting in a decrease in the porosity and an increase in the density compared to the control sample. The addition of hybrid nanomaterials leads to a decrease in the porosity and resulting in a slight increase in the density as shown in Figure (10). These results are in agreement with those obtained by Liu et al. [37].

4-2-2 Compressive Strength

In Table (5), the test results of the compressive strength for all mixes at 7 and 28 days are presented. Three measurements samples were used to get the average of each result. From Figure (11), it can be noticed that the compressive strength of concrete increases when replacing the cement with nanomaterials. Among all mixes, the NMK mix showed the highest increase in compressive strength by 22.7 %. This may be attributed to the improvement of the cementitious materials by the reaction of NMK and CH generated by cement hydration to produce extra C-S-H and hexagonal hydrated calcium aluminate (mostly C_4AH_{13}) [38]. Additionally, SEM images confirmed the main contribution of the pozzolanic interaction between the various materials, as shown in Figure (21). The following is an explanation of how the addition of NMK improved the chemical and physical properties: The microstructure of cement paste became denser when NMK's ultra-fine particles filled in the cement's pores. Excess calcium silicate hydrate (C-S-H) produced by the pozzolanic reaction of NMK with free lime released during the hydration process is deposited in the pore system, improving the mechanical properties [18]. These results were confirmed by another research [21]. Moreover, the compressive strength of concrete with NS is higher than the control samples by 10% due to the pozzolanic reaction of NS as in [39- 41]. Tawfik et al. [12], studied the effect of NC and NS on the properties of concrete, they found that when using NC up to 6%, NS up to 3% and hybrid of NS and NC, it enhances the mechanical properties of concrete. The increment in the compressive strength of NC samples as compared to the control samples due to the additional surfaces of NC. For the heterogeneous nucleation of hydration products such as calcium hydroxide (CH), calcium-silicate-hydrate (C-S-H), and other hydration products, it may be supplying additional sites and locations. Additionally, the uniform distribution of ceramic grains reduces the distance travelled by ions from the active minerals to the nucleating sites. Those effects have the power to effectively boost cement hydration rates and heterogeneous nucleation densities. Science, the NC pozzolanic reactions result in stronger binding phases that enhance contacts between cement hydrates and ceramic grain particles. The mechanical attitude of the NC-cement materials is simultaneously affected by those chemical-physical influences [42]. Binary mixes (NS+NC or NS+NMK) showed a small increase compared with that of the control sample. This is due to the double effect of nano silica and nano ceramic or nano silica and nano metakaolin on the substantial properties.

4-2-3 Tensile Strength

As illustrated in Figure (12), it is noted that the tensile strength of NMK samples exhibits the highest value. In fact, the NMK uses two mechanisms to increase the tensile strength of hardened cement mortar. The first mechanism involves the effect of NMK as filler packing intermittent voids inside the skeleton of the hardened microstructure of cement mortar, so improving both its density and strength. The pozzolanic effect is the second mechanism. In the NS samples, the pozzolanic reaction between calcium hydroxide and amorphous silica is slow during extended moist curing, but it responds quickly in an alkaline environment, such as the pore solution of freshly mixed Portland cement mortar. It is obvious that NMK and portlandite or calcium-hydroxide (CH) can react and result in the formation of additional C-S-H that is identical in composition and structure to that produced by the hydration of Portland cement. (18). Much research has confirmed that using NS in concrete fills the pores in the concrete matrix while also acting as a nano-reinforcement and filling agent and enhancing the tensile strength, [43- 46]. Moreover, the use of NC in concrete exhibited a higher tensile strength compared to that of the control mix as found in the work of Tawfik et al. [12].

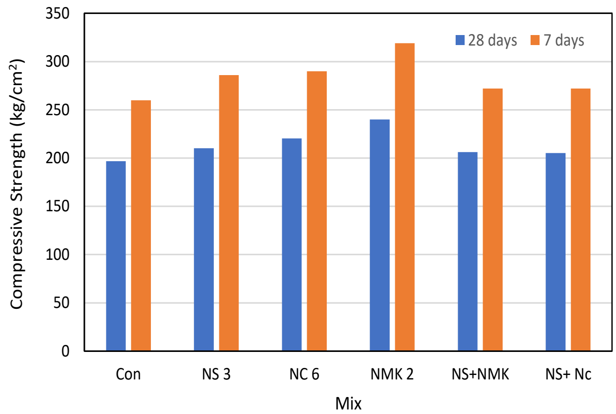

Fig. (10): Compressive Strength at 7 and 28 days

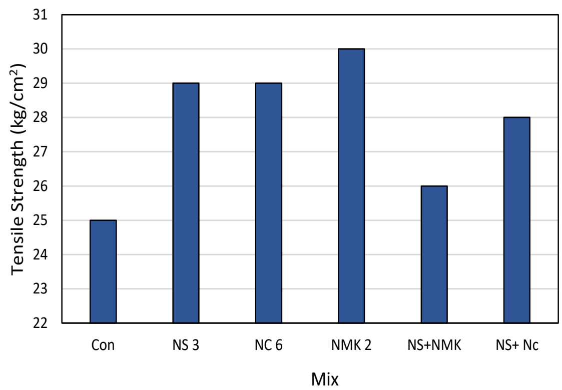

Fig. (11): Tensile Strength at 28 days

4-3 Physical Properties of Concrete

Table (5) provides a summary of the test results for the water absorption of all mixes at 28 days. The average of three measurements is used to calculate each value. It can be observed that using nanomaterials as a replacement of cement decreased voids, pores, and improved the homogeneous characteristics of concrete in all mixes compared with the control mix. The percentage of decreases in water absorption were [11.41%, 14.28%,20%, 25.71% and 22.85%] at NS, NC, NMK, Ns+NMK, and NS+NC mixes respectively as shown in Figure (13). This decrease is attributed to the filler effects of nanoparticles and their pozzolanic activity. One more observation is that the pozzolanic reaction and the filler effect of the nanoparticles have improved the interfacial transition zone in concrete. These findings confirm the results of Nazari and Riahi [47].

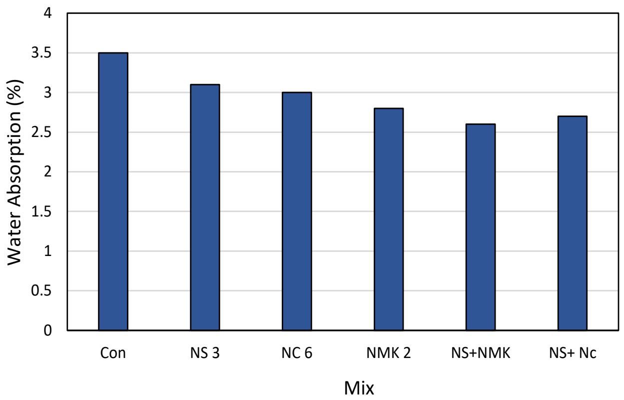

Fig. (13): Water Absorption of all Mixes

4-4 Experimental and Theoretical results of linear attenuation coefficient

Results of gamma attenuation are illustrated in Table (5) and Figures (14-16). The results include sample thickness (X), $\mu \times X = \ln (Io/I)$, linear attenuation coefficient (μ, cm^{-1}), and density. The values of μ in Table (5) are the average of five different tests conducted on five different thicknesses of the same mix. The experimental results and MCNP5 calculations for control and samples containing nano materials are presented in Figures (14 and 15). It is clear from the Figures that the penetration probability of radiation is higher for control samples than for samples containing nanomaterials. This means that nanomaterials improve the shielding properties of concrete [48]. Figure (15) shows the comparison between the simulation results of linear attenuation coefficient using MCNP code, XCOM program and experimental values. From the experimental work, the highest average linear attenuation coefficient was found in (NMK) samples. The gamma attenuation for concrete with nano metakawlin is 0.196 cm^{-1}, concrete with nano ceramic is 0.183 cm^{-1}, concrete with nano silica is 0.179 cm^{-1}, (NS+NC) and (NS+NMK); concrete with hybrid nano materials; is 0.178 and 0.179 cm^{-1} respectively, and, finally, in the common concrete without nanomaterial (control concrete) was 0.176 cm^{-1}. These values are compatible with those reported in earlier publications [48-49]. The simulation linear attenuation coefficient was calculated using equation 1, by applying the intensity ratio (I/Io) obtained from the results of the MCNP5 run and XCOM program. The interpretation of the results of μ yields that when the density increases due to incorporating nanomaterial in concrete, the linear attenuation coefficient increases. The highest increase in attenuation coefficient was in NMK concrete due to the fineness of NMK than the other nanomaterials which were used in this research. The NMK fills the pores and voids in cement paste that leads increasing the density. The validation of the MCNP model has been verified by comparing experimental and calculated linear attenuation coefficient as shown in Figure (16). The relative difference between the experimental and the MCNP values is found to be about 1.553% higher than experimental results, this may be due to many reasons which may include the non-homogeneity of the material compositions, the tolerance in the thicknesses of the samples, and statistical errors in counting rates and position-related errors. All these sources of errors could be avoided in simulation models and XCOM program. Figure (17) demonstrates the relation between the sample thickness and ln(lo/l). The relation is directly proportional considering all control and nano mixes.

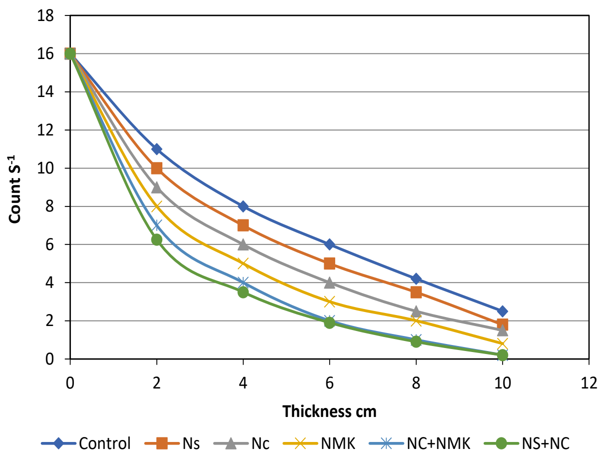

Fig. (14): Experimental results for all mixes

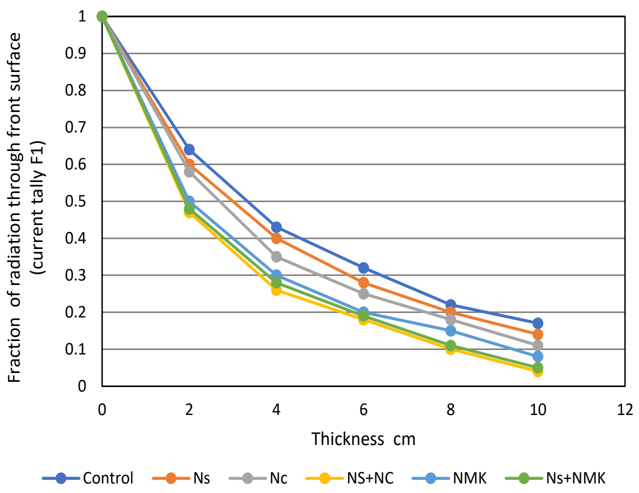

Fig. (15): Monte Carlo simulation for all mixes

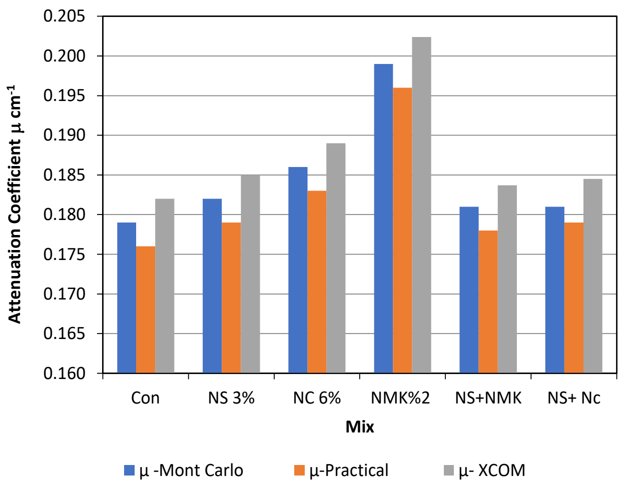

Fig. (16): Comparision between experimental and theoritical work for all mixes

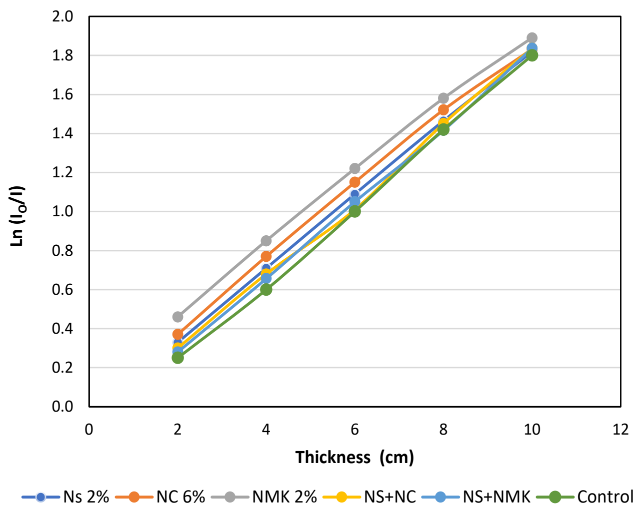

Fig. (17): The relation between sample thickness and ln (Io/I)

The validation of the MCNP model has been verified by comparing the experimental and calculated linear attenuation coefficient as shown in Figure (7).

4-5 Results of XRD Analyses

X-ray diffractograms of concrete with nano particles hydrated for 28 days are shown in Figure (18). The Figure shows that the concrete containing nano silica (NS concrete) has less intensity diffraction lines corresponding to C-H and more intensity diffraction lines with characteristics for C-S-H compared to the corresponding lines of the control mix). This is caused by the pozzolanic interaction between the nano silica and C-H resulted in more C-S-H phases [39]. Furthermore, the same results were shown in concrete containing NC or NMK when compared with the control sample, the intensity of the CH peak decreased and remarkably increased the intensity of C-S-H in each mix with the incorporating of NC or NMK. This is due to the acceleration growth of the C-S-H by the nucleation effect of the NC and NMK and the pozzolanic reaction which gets more C-S-H as described in other studies [26, 33]. The denser the concrete is, the greater intensity of diffraction lines for C-S-H. Indirectly, it will improve the properties of the concrete as shown in NMK concrete as it has a higher mechanical property when compared with other samples as described in sec 4-2 and in another work [40]. The intensity of diffraction lines of characteristics for (Q) quartz appeared for NS at (2θ) = 22.1, for NC at (2θ) = 26.8, and for NMK at (2θ) = 26.88, this agreed with the XRD analysis of nano particles as shown in Figure (2). Figures (19 and 20) show that the diffraction lines corresponding to C-S-H in (NS+NC) was less than those of the corresponding lines of the NS or NC mix and slightly higher intensity of the diffraction lines of characteristics for C-H for (NS+NC) than those of the corresponding lines of the NS or NC. Additionally, the same behavior occurred when mixing the NS and NMK, which reflected the dual effect of nanomaterials as illustrated in mechanical properties.

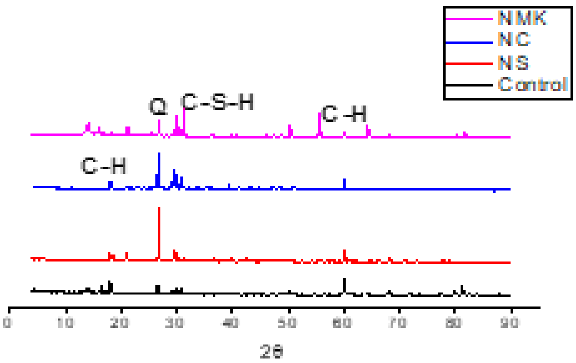

Fig. (18): XRD pattern of concrete containing different nano materials

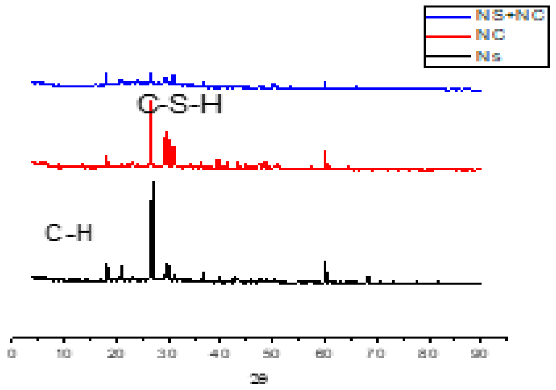

Fig. (19): XRD pattern of concrete containing NS+NC

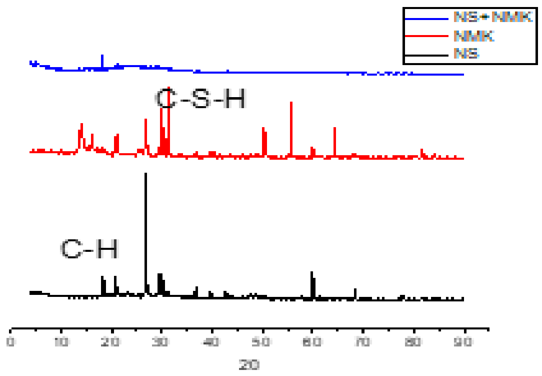

Fig.(20): XRD pattern of concrete containing NS+NMK

4-4 Microstructure

The morphological features changes of concrete containing nanomaterials were examined to analyze the effects of the nanomaterials compared with the control concrete and the results are shown in Figure (21). In Figure (21-a), the microstructure of the control sample is presented, there are more unhydrated cement particles and low C-S-H crystals, furthermore, it has a high ratio of porosity and less homogeneity compared to that samples with nanoparticles. It is readily visible in Figure (21-b) that adding nano silica results in the reduction of the amount of cumulative incursion related to porosity compared to the control sample. Porosity decreases with the addition of nano silica compared with the control sample. It can be attributed to the finesse of nano silica which fills the pores and leads to denser matrix. In addition, it is notable that incorporating the nano ceramic, makes the sample denser than the control sample, and thus, the initial voids, flaws, and gaps between particles are filled with new hydrations progressively (C-S-H) from pozolanic reaction as shown in Figure (21-C). The microstructure of the concrete containing NMK appeared to be much denser matrix than the control sample, NS, and NC samples which is attributed to the high fineness of NMK particles which can fill the pores between cementitious material particles in the microstructure as shown in Figure (21-D). Furthermore, The NMK acts as a link between micro-cracks to prevent the formation of new cracks in concrete and enhance its mechanical properties. Additionally, NMK forms a more compact structure. These findings are compatible with other studies [50, 51]. The microstructure of the sample containing NS+NC appeared quite dense and compact with relatively fewer capillary pores as compared to the control sample. It could be clearly observed that the pores and the number of voids are reduced as a result of adding NS or NC or NMK. It is also clear that the nanoparticles enhance the concrete's fine pores. This could explain how nanoparticles contributed to improve the mechanical properties indicated in Sec. 4.2.

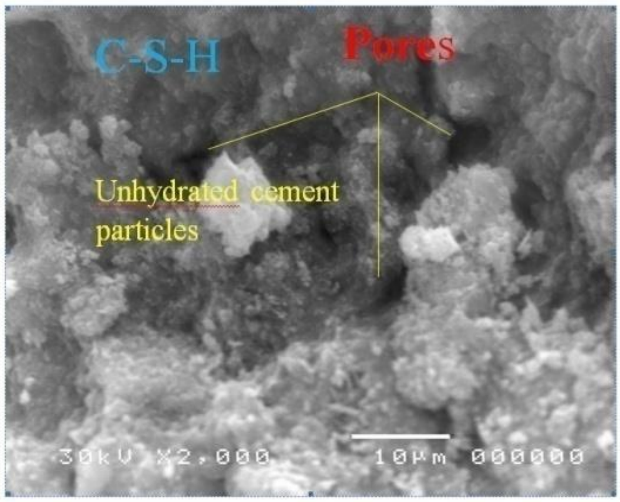

(a) Control Concrete

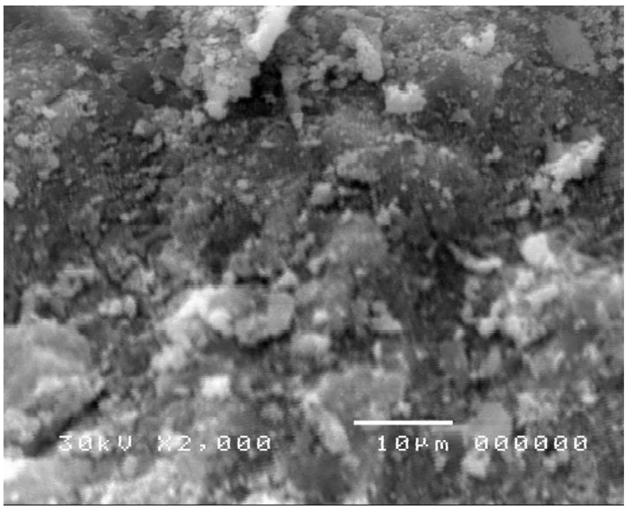

(b) Concrete with NS

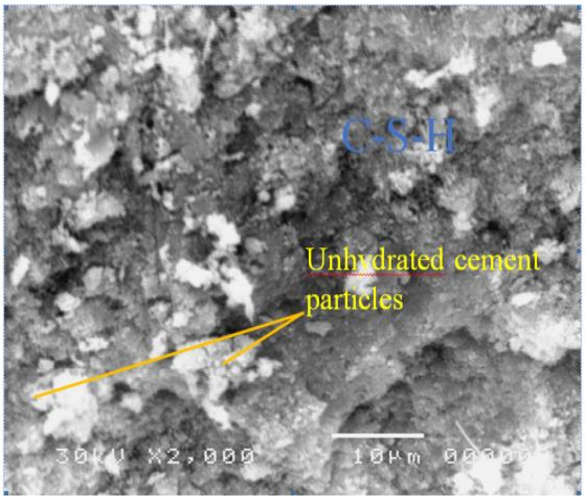

(C) Concrete with NC

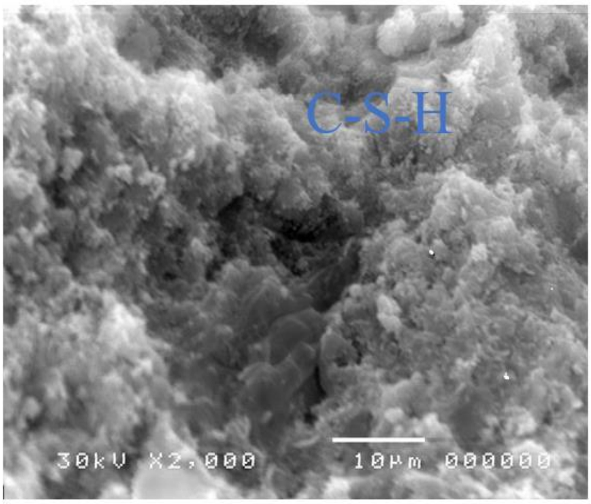

(D) Concrete with NMK

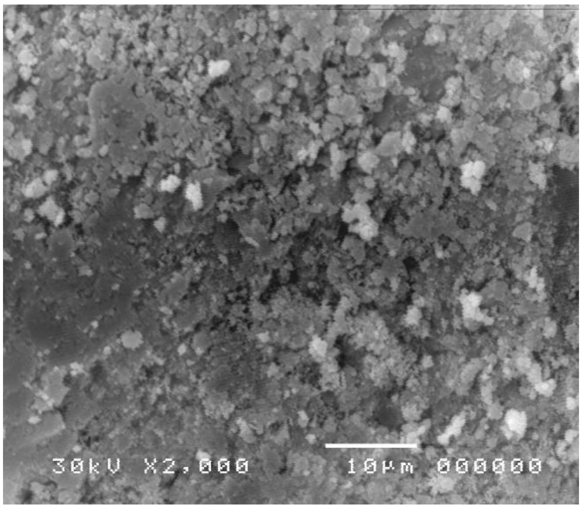

(E) Concrete with NS+NC

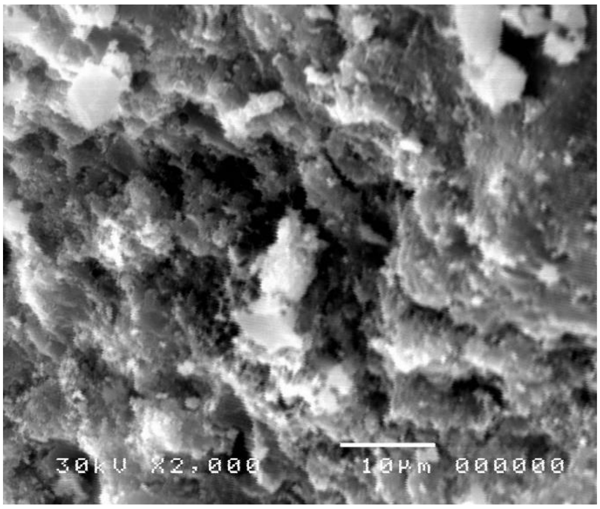

(F) Concrete with NS+NMK

Fig. (21): Microstructure of all mixes

5- CONCLUSION

The present work shows the simulation of linear attenuation coefficient with the Mont Carlo and XCOM program of concrete containing nanomaterials NS, NC or NMK and their hybridization comparing with the experimental results. The nanomaterials were added at percentages of 3%, 6% and 2% as a replacement of cement weight for NS, NC and NMK respectively. Moreover, the physical, mechanical properties, SEM and XRD of the concrete were investigated. Based on the results of the laboratory tests and the theoretical studies, the following conclusions can be drawn:

1- The gamma attenuation coefficient results showed that the highest increase value in μ of the Monte Carlo simulation was in concrete containing NMK with a percentage increase of 7.08% followed by: NC with 2.16%, NS with 1.6%. The least increase in μ was found in the hybrid nano concrete mixes.

2- The relative difference between the experimental and the MCNP values of attenuation coefficient was found to be about 1.553% higher than the experimental, while the relative difference between XCOM and MCNP was about 1.658%.

3- The nanomaterials increase the shielding of the concrete and lead to a proper filling characteristic and hence increasing the concrete density. The increase in attenuation coefficient directly leads to a decrease in the designed concrete thickness.

4- Water absorption decreased due to the use of nanoparticles. The highest reduction in water absorption was 25.7 % measured in the NS+NMK samples.

5- Using nanomaterials improved the compressive strength of concrete for all mixes to some value when compared to the control mix. It increases by 10%, 11.5%, 22.7%, 4.6% and 4.6% for NS, NC, NMK, NS+ NMK, and NS+NC respectively at the age of 28 days. Furthermore, the increases in tensile strength were 16%,16%,20%,4% and 8% for NS, NC, NMK, NS+NMK, and NS+NC respectively at the same nano ratio.

6- Microstructure analysis showed that the incorporating the NS, NC and NMK nanoparticels in the concrete led to good hydration product as well as filling effect of voids in cement matrix thus making the microstructure of the cement paste more denser comparing with the control mix.

7- Pores from the image processing SEM images showed a significant decrease in the percentage of pores between the control mix and the mixes containing nanomaterials. The highest pores reduction analyzed among all mixes was attributed to the addition of 2% NMK.

8- Based on the XRD analysis, it can be concluded that there is a significant effect of nanomaterial on the tested samples.

6- REFERENCES

[1] Sayed Nooruddin, Syed Shah Maqdoom Hussaini, Syed Umair, Akshay Belgar, Prof. Sujeet Patil (2019). Strength of nano concrete using nano silica. International Journal of Engineering Research & Technology (IJERT) http://www.ijert.org ISSN: 2278-

[2] Nazari A, Riahi S., "The effects of SiO2 nanoparticles on physical and mechanical properties of high strength compacting concrete", Composites Part B, 42(3),570–578 (2011).

[3] Stefanidou M., Papayanni I., "Influence of nano-SiO2 on the Portland cement pastes", Composites. Part B: Engineering, 43, 2706-2712 (2012)

[4] Reddy, Avuthu Narender, S. Priyanka, and P. Mounika. "The Effect of Nano Silica on Mechanical Properties of Concrete." Internat. Res. J. Applied Sci. 1 (2019): 36-40.

[5] Shaikh, Faiz Uddin Ahmed, Heasam Odoh, and Andrew B. Than. "Effect of nano silica on properties of concretes containing recycled coarse aggregates." Proceedings of the Institution of Civil Engineers-Construction Materials 168, no. 2 (2015): 68-76.

[6] MY, M. I., Ramad hansyah, P. J., MH, W. I., & Fadzli, M. N. (2015). Utilization of nano silica as cement paste in mortar and porous concrete pavement. Adv. Mater. Res., 1113, 135-139.

[7] Norhasri, MS Muhd, M. S. Hamidah, and A. Mohd Fadzil. "Applications of using nano material in concrete: A review." Construction and Building Materials 133 (2017): 91-97.

[8] Nazari A, Riahi S., "The effects of SiO2 nanoparticles on physical and mechanical properties of high strength compacting concrete", Composites Part B, 42(3),570–578 (2011).

[9] Sololev K., "Engineering of Silica nanoparticles for optimal performance in nano cement-based materials", Nano Technology in Construction, Proceedings of the NICOM3, Prague, 139-148 (2009).

[10] Peng Zhang (2021) A Critical Review on Effect of Nanomaterials on Workability and mechanical properties of high-performance concrete

[11] Ghafari, E., Costa, H., Júlio, E., Portugal, A., & Durães, L. (2014). The effect of nanosilica addition on flowability, strength and transport properties of ultra-high-performance concrete. Materials & Design, 59, 1-9.

[12] Tawfik, T. A., Metwally, K. A., El-Beshlawy, S. A., Al Saffar, D. M., Tayeh, B. A., & Hassan, H. S. (2020). Exploitation of the nanowaste ceramic incorporated with nano silica to improve concrete properties. Journal of King Saud University-Engineering Sciences. https://doi.org/10.1016/j.jksues.2020.06.007.

[13] Ibrahim K.I.M., Al-Tersawy S. H., "The hybrid effect of micro and nano silica on the properties of normal and high strength concrete", IOSR Journal of Mechanical and Civil Engineering, 14 (4), 62-72 (2017).

[14] Siddique, R., & Klaus, J. (2009). Influence of metakaolin on the properties of mortar and concrete: A review. Applied Clay Science, 43(3-4), 392-400. doi: 10.1016/j.clay.2008.11.007.

[15] Shen, P., Lu, L., Chen, W., Wang, F., & Hu, S. (2017). Efficiency of metakaolin in steam cured

high strength concrete. Construction and building materials, 152, 357- 366. http://dx.doi.org/10.1016/j.conbuildmat.2017.07.006.

[16] Güneyisi, E., Gesoğlu, M., & Mermerdaş, K. (2008). Improving strength, drying shrinkage, and pore structure of concrete using metakaolin. Materials and structures, 41(5), 937-949.

[17] Fadzil, M. A., Nurhasri, M. M., Norliyati, M. A., Hamidah, M. S., Ibrahim, M. W., & Assrul, R. Z. (2017). Characterization of Kaolin as Nano Material for High Quality Construction. In MATEC Web of Conferences (Vol. 103, p. 09019). EDP Sciences

[18] Morsy, M. S., Alsayed, S. H., & Aqel, M. (2010). Effect of nano-clay on mechanical properties and microstructure of ordinary Portland cement mortar. International Journal of Civil & Environmental Engineering IJCEE-IJENS, 10(01), 23-27.

[19] Shoukry, H., Kotkata, M. F., Abo-EL-Enein, S. A., Morsy, M. S., & Shebl, S. S. (2016). Enhanced physical, mechanical and microstructural properties of lightweight vermiculite cement composites modified with nano metakaolin. Construction and Building Materials, 112, 276-283. http://dx.doi.org/10.1016/j.conbuildmat.2016.02.209

[20] Shoukry, H., Kotkata, M. F., Abo-el-Enein, S. A., & Morsy, M. S. (2013). Flexural strength and physical properties of fiber reinforced nano metakaolin cementitious surface compound. Construction and Building Materials, 43, 453-460.

[21] Nithya, N., Sarathy, R. V., Raj, B., & Raman, K. R. (2015). Experimental study on strength and durability properties of concrete with nano metakaolin. International Journal of Engineering and Management Research (IJEMR), 5(2), 840-843.

[22] Xie, J., Zhang, H., Duan, L., Yang, Y., Yan, J., Shan, D., & Zhang, Y. (2020). Effect of nano metakaolin on compressive strength of recycled concrete. Construction and Building Materials, 256, 119393. DOI.org/10.1016/j.conbuildmat.2020.119393.

[23] Khalil, K. A. (2012). Advanced sintering of nano-ceramic materials. Ceramic Materials-Progress in Modern Ceramics, 65-82.

[24] C Thomas, S., Kumar Mishra, P., & Talegaonkar, S. (2015). Ceramic nanoparticles: fabrication methods and applications in drug delivery. Current pharmaceutical design, 21(42), 6165-6188.

[25] Li, L., Liu, W., You, Q., Chen, M., & Zeng, Q. (2020). Waste ceramic powder as a pozzolanic supplementary filler of cement for developing sustainable building materials. Journal of Cleaner Production, 259, 120853.

[26] Singh, Vishwanath P., A. M. Ali, N. M. Badiger, and A. M. El-Khayatt. "Monte Carlo simulation of gamma ray shielding parameters of concretes." Nuclear Engineering and Design 265 (2013): 1071-1077.

[27] Khaldari, R., Mesbahi, A., & Kara, U. (2016). Monte Carlo calculation of shielding properties of newly developed heavy concretes for megavoltage photon beam spectra used in radiation therapy. Iranian Journal of Medical Physics, 13(4), 250-260

[28] D. C. MCDOWALL, in "Proc. of Information Exchange in Results of Concrete Irradiation Programs," edited by H. Bezler (Commission of the European Communities, Luxembourg) p. 55.

[29] Aziz, F., Panitra, M., & Rivai, A. K. (2018). Synthesis and Monte Carlo Simulation of Improved Concrete Composites for Enhanced X-Ray/Gamma Ray Radiation Shielding. International Journal of Technology, 2018(4), 695-706.

[30] ESS 2421/2005—Egyptian Standard Speciication, Cement— Physical and Mechanical Tests.

[31] ESS1109/2002, Egyptian Standard Specification, "Aggregate for Concrete".

[32] ESS 1658/2006—Egyptian Standard Specification, "Testing of Concrete".

[33] American Society for Testing and Materials C 642, (1997), "Standard Test Method for Density, Absorption and Voids in Hardened Concrete," 3 pages.

[34] S. Yıldırım, A.B. Tugrul, B. Buyuk and E. Demir, Gamma Attenuation Properties of Some Aluminum Alloys 2015

[35] XCOM, N. (2018). Element/Compound/Mixture.

[36] Norhasri, M. M., Hamidah, M. S., Fadzil, A. M., & Megawati, O. (2016). Inclusion of nano metakaolin as additive in ultra-high-performance concrete (UHPC). Construction and Building Materials, 127, 167-

[37] Liu Xin He*, Xiaowei Deng*, Yuyou Wu*, Zhoulian Zheng " Application of nanomaterials in ultra-high-performance concrete" 2020

[38] Zhan, P. M., He, Z. H., Ma, Z. M., Liang, C. F., Zhang, X. X., Abreham, A. A., & Shi, J. Y. (2020). Utilization of nano-metakaolin in concrete: A review. Journal of Building Engineering, 30, 101259. DOI: 10.1016/j.jobe.2020.101259

[39] Reddy, A. N., Priyanka, S., & Mounika, P. (2019). The effect of nanosilica on mechanical properties of concrete. Int'l Res J Appld Sci, 1(1), 36-40.

[40] Aleem, S. A. E., Heikal, M., & Morsi, W. M. (2014). Hydration characteristic, thermal expansion and microstructure of cement containing nano-silica. Construction and Building Materials, 59, 151-160.

[41] Yusak, M. I. M., Jaya, R. P., Hainin, M. R., & Wan, M. H. (2016). A review of microstructure properties of porous concrete pavement incorporating nano silica. ARPN J. Eng. Appl. Sci, 11, 11832-11835.

[42] Lavat, A. E., Trezza, M. A., & Poggi, M. (2009). Characterization of ceramic roof tile wastes as pozzolanic admixture. Waste management, 29(5), 1666-1674.

[43] Zhuang, C., & Chen, Y. (2019). The effect of nano-SiO2 on concrete properties: a review. Nanotechnology Reviews, 8(1), 562-572.

[44] Zhang A., Ge Y., Yang W.C., Cai X.P., Du Y.B., Comparative study on the effects of nano-SiO2 nano-Fe2O3 and nano-NiO on hydration and microscopic properties of white cement, Constr. Build. Mater., 2019, 228,

116767.10.1016/j.conbuildmat.2019.116767

[45] Nili M., Ehsani A., Investigating the effect of the cement paste and transition zone on strength development of concrete containing nanosilica and silica fume, Mater. Des., 2015, 75, 174-183.

[46] Fallah S., Nematzadeh M., Mechanical properties and durability of high-strength concrete containing macro-polymeric and polypropylene fibers with nano-silica and silica fume, Constr. Build. Mater., 2017, 132, 170-187.

[47] Nazari A, Riahi S., "The effects of SiO2 nanoparticles on physical and mechanical properties of high strength compacting concrete", Composites Part B, 42(3),570–578 (2011).

[48] Elsharkawy, E. R., & Sadawy, M. M. (2016). Effect of gamma ray energies and addition of nano-SiO2 to cement on mechanical properties and mass attenuation coefficient. IOSR J. Mech. Civ. Eng., 13(6), 17-22.

[49] Al-Tersawy, S. H., El-Sadany, R. A., & Sallam, H. E. M. (2021). Long-term behavior of normal weight concrete containing hybrid nanoparticles subjected to gamma radiation. Archives of Civil and Mechanical Engineering, 21(1), 1-18.

[50] Xiaoyu, F. Yingfang, L. Haiyang, The compressive behavior of cement mortar with the addition of nano metakaolin, Nanomater. Nanotechnol. 8 (6) (2018) 1–7.

[51] M.S. Morsy, Y. Al-Salloum, T. Almusallam, et al., Effect of nano-metakaolin addition on the hydration characteristics of fly ash blended cement mortar, J. Therm. Anal. Calorim. 116 (2) (2014) 845–852.